Chemosphere 179 (2017) 20–28

Contents lists available at ScienceDirect

Chemosphere

journal homepage: www.elsevier.com/locate/chemosphere

Adsorption of emerging contaminant metformin using graphene oxide

Shuai Zhu [a, b], Yun-guo Liu [a, b, *], Shao-bo Liu [c, d, **], Guang-ming Zeng [a, b], Lu-hua Jiang [a, b], Xiao-fei Tan [a, b], Lu Zhou [a, b], Wei Zeng [a, b], Ting-ting Li [a, b], Chun-ping Yang [a, b]

[a] College of Environmental Science and Engineering, Hunan University, Changsha 410082, PR China
[b] Key Laboratory of Environmental Biology and Pollution Control (Hunan University), Ministry of Education, Changsha 410082, PR China
[c] School of Architecture and Art, Central South University, Changsha 410082, PR China
[d] School of Metallurgy and Environment, Central South University, Changsha 410083, PR China

HIGHLIGHTS

- Rapid and efficient removal of metformin can be achieved during the adsorption process.
- Sorption kinetic, isothermal and thermodynamic characteristics of metformin are explored.
- The adsorption capacity of GO for metformin is influenced in the presence of NaCl and background electrolyte.
- The adsorption mechanism is believed to be so-called π−π interactions and hydrogen bonds between GO and metformin.

ARTICLE INFO

Article history:
Received 16 November 2016
Received in revised form
12 March 2017
Accepted 16 March 2017
Available online 27 March 2017

Handling Editor: Patryk Oleszczuk

Keywords:
Emerging contaminants
Pharmaceutical
Metformin
Graphene oxide
Adsorption

ABSTRACT

The occurrence of emerging contaminants in our water resources poses potential threats to the livings. Due to the poor treatment in wastewater management, treatment technologies are needed to effectively remove these products for living organism safety. In this study, Graphene oxide (GO) was tested for the first time for its capacity to remove a kind of emerging wastewater contaminants, metformin. The research was conducted by using a series of systematic adsorption and kinetic experiments. The results indicated that GO could rapidly and efficiently reduce the concentration of metformin, which could provide a solution in handling this problem. The uptake of metformin on the graphene oxide was strongly dependent on temperature, pH, ionic strength, and background electrolyte. The adsorption kinetic experiments revealed that almost 80% removal of metformin was achieved within 20 min for all the doses studied, corresponding to the relatively high k_1 (0.232 min^{-1}) and k_2 (0.007 g mg^{-1} min^{-1}) values in the kinetic models. It indicated that the highest adsorption capacity in the investigated range (q_m) of GO for metformin was at pH 6.0 and 288 K. Thermodynamic study indicated that the adsorption was a spontaneous ($\Delta G^0 < 0$) and exothermic ($\Delta H^0 < 0$) process. The adsorption of metformin increased when the pH values changed from 4.0 to 6.0, and decreased adsorption were observed at pH 6.0–11.0. GO still exhibited excellent adsorption capacity after several desorption/adsorption cycles. Besides, both so-called π−π interactions and hydrogen bonds might be mainly responsible for the adsorption of metformin onto GO.

1. Introduction

Pharmaceutical and Personal Care Products (PPCPs) were a series of compounds including analgesics, antibiotics, contraceptives, lipid regulators, in addition to the active ingredients in soaps, detergents, perfumes, and skin, hair, and dental care products (Rice and Mitra, 2007). In recent years, their increasing consumption and adverse effects on ecological or human body have been attained extensive attention. The emission of these emerging contaminants has emerged as an environmental problem and rather poor wastewater management could not effectively eliminate these compounds (Terzić et al., 2008). Therefore, there is a widespread demand that this kind of contamination requires effective

* Corresponding author. College of Environmental Science and Engineering, Hunan University, Changsha 410082, PR China.
** Corresponding author. School of Architecture and Art Central South University, Central South University, Changsha 410082, PR China.
E-mail addresses: liuyunguo_hnu@163.com (Y.-g. Liu), liushaobo23@aliyun.com (S.-b. Liu).

http://dx.doi.org/10.1016/j.chemosphere.2017.03.071
0045-6535/

elimination.

Metformin has become a worldwide first-line pharmaceutical for type 2 diabetes mellitus since the late 1950s (Viollet et al., 2012), the medicinal use was well characterized, but the effect it had on the environment was still uncertain. It was found that there were some threats in intersex gonads in male fish, fecundity and the overall size of male fish after exposing fathead minnows in wastewater effluent with metformin (*Pimephales promelas*), and the juvenile *Pimephales promelas* were more susceptible to the estrogenic effects of metformin than older, sexually mature male one (Niemuth and Klaper, 2015; Crago et al., 2016). Metformin was not structurally hormone-like chemical compound, and could not cause estrogenic activity (Escher et al., 2011). However, it has been proved that metformin was an effective medicine to treat endocrine disorder polycystic ovarian syndrome (PCOS) (Tang et al., 2012). The results suggested that metformin might be a potential endocrine disruptor in the environment (Niemuth and Klaper, 2015). Thus, metformin would be one of the nontraditional endocrine disrupting chemicals (EDCs) in the environment. Despite a large conversion in wastewater treatment plants (WWTPs) before discharge, metformin was still one of the most abundant pharmaceuticals found in WWTP effluent and surface-waters, and it could usually reach 6 tons per year in individual WWTPs of urban areas (Blair et al., 2013; Oosterhuis et al., 2013). Therefore, metformin has become an emerging contaminant in the environment. It is necessary to find a way to decontaminate metformin.

Adsorption has been proved to be an excellent and promising technique due to its low expenses, accessibility, excellent performance, and environmentally benignity. In recent years, various materials have been widely applied to the elimination of various contaminants, such as powdered activated carbon (PAC) (Yoon et al., 2003), ion exchange resin (Gupta et al., 2004; Wang et al., 2016), carbon nanotubes (Yao et al., 2010), chitosan (Hu et al., 2011a), bottom ash (Mittal et al., 2009a, 2009b, 2010a, 2010b), activated carbon (Gupta et al., 1998; Gu et al., 2009), biochar (Tan et al., 2015, 2016, 2017) and organic resin (Lu et al., 2016). However, these sorbents suffered the problem of either low sorption capacities or high-cost. Thus, there is a strongly desire to search for a high-performance, low-cost adsorbent. Graphene oxide (GO), a single atomic layer material derived from graphene, has inspired huge interests in adsorption, photocatalytic degradation and sensor, due to its excellent physical-chemical properties and high specific surface area (theoretical value of 2620 $m^2\ g^{-1}$) (Zhao et al., 2011b; Chang and Wu, 2013; Hu et al., 2016). It has confirmed that GO could be a promising adsorbent, because it had large surface area and abundant surface oxygen-containing groups (Hu et al., 2014a; Wu et al., 2017). In previous study, GO was used as an adsorbent to remove metal ions (copper, zinc, cadmium and lead), the maximum adsorption capacity of GO for Cu(II), Zn(II), Cd(II) and Pb(II) could reach 294, 345, 530, and 1119 mg g^{-1}, respectively (Sitko et al., 2013). It was demonstrated that GO could act as a good adsorbent in adsorbing tetracycline antibiotics from aqueous solution (Gao et al., 2012). GO could also be successfully applied for the removal of aniline (Fakhri, 2017), 17β-estradiol (Jiang et al., 2016). Moreover, GO could be an efficient adsorbent for the removal of various dyes such as methylene blue, methyl violet and Basic Red 12 (Ramesha et al., 2011; Moradi et al., 2015). It was reported that metformin was an emerging contaminant in the environment (Niemuth and Klaper, 2015; Crago et al., 2016), and effective removal was needed. Unfortunately, there were very little data available about the elimination of metformin, few articles about the reduction of metformin had been reported (Blair et al., 2013; Kim et al., 2014; Neamţu et al., 2014; Kyzas et al., 2015; Cui and Schröder, 2016), and the application of graphene oxide as an adsorbent in the removal of metformin from aqueous solution was still scarce.

In this study, GO was studied for the first time to remove metformin from aqueous solution and characterized by scanning electron microscope (SEM), transmission electron microscope (TEM), X-ray diffraction (XRD), Fourier transform infrared spectroscopy (FTIR), X-ray photoelectron spectroscopy (XPS), Brunauer-Emmett-Teller (BET) and zeta potential to investigate its adsorption behaviors. Batch adsorption experiments were carried out to explore the effects of contact time, concentration, temperature, pH, and ionic strength on the removal of metformin by GO. The effects of electrolyte anions (Cl^-, NO_3^-, SO_4^{2-} and PO_4^{3-}) and electrolyte cations (Na^+, K^+, Mg^{2+} and Ca^{2+}) in aqueous solutions on the adsorption of metformin onto GO were also investigated.

2. Materials and methods

2.1. Materials

Metformin (97%) were purchased from Acceia ChemBio Co., Ltd and graphite powder was obtained from Tianjin Kermel Chemical Regent Ltd. All chemicals including $K_2S_2O_8$, P_2O_5, H_2SO_4, $NaNO_3$, $KMnO_4$, H_2O_2, NaCl, Na_3PO_4, KCl, Na_2SO_4, $MgCl_2$, $CaCl_2$ and HCl were supplied by Shanghai Chemical Corp. All compounds used in the experiment were analytical grade without further purification. All the solutions were prepared using high purity water (18.25 MΩ cm^{-1}) from a Millipore Milli-Q water purification system. A stock solution (40 mg L^{-1}) of metformin was prepared by dissolving 42 mg of metformin (97%) in 1 L of Milli-Q water. The working solution of desired metformin concentrations used in the following experiments was obtained by diluting the stock solution.

GO was prepared by using modified Hummers method from the natural graphite powder (Jiang et al., 2016). Briefly, 6 g graphite powder was firstly oxidized by 24 ml concentrated H_2SO_4 (98%), 5 g $K_2S_2O_8$ and 5 g P_2O_5, and stirred at 353 K for 4.5 h. Then, 1 L of Milli-Q water was added and left overnight. The mixture was washed thoroughly and dried under vacuum at 333 K. Next, 240 ml 273 K concentrated H_2SO_4 (98%), 30 g $KMnO_4$ and 5 g $NaNO_3$ were slowly added to oxidize the preoxidized graphite and stirred below 293 K for 4 h. Then, the reaction was carried out at 308 K for 2 h. Next, 500 ml Milli-Q water was added slowly and the mixture was stirred for another 6 h at 363 K. After that, 40 ml H_2O_2 (30%) was used to eliminate the surplus MnO_4^- and stirred for 2 h at room temperature. The products were finally washed by 10% (v/v) HCl and water several times. The resulting solution was sonicated for 2 h and freeze dried for further use.

2.2. Characterization of GO

The surface morphologies and structures of GO were observed by scanning electron microscope (SEM, JSM-7001F, Japan) and transmission electron microscope (TEM, JEM-3010, Japan). The fourier transform infrared spectroscopy (FTIR) of GO was conducted by using a Nicolet 5700 FT-IR Spectrometer (Thermo Scientific). The surface elemental composition analyses of GO were characterized based on the X-ray photoelectron spectroscopy (XPS) (Thermo Fisher, USA). The Brunauer-Emmett-Teller (BET) specific surface area of GO was measured by using automatic surface analyzer (Quantachrome, USA). The X-ray diffraction (XRD) patterns of GO was obtained by an X-ray diffractometer (Rigaku D/max-2500, Japan) with Cu Kα radiation (k = 1.541 Å). The zeta potentials of GO in water solutions at pH 4.0–11.0 (adjusted by NaOH or HCl) was detected by a zeta potential meter (Zetasizer Nano-ZS90, Malvern).

2.3. Batch adsorption procedures

Batch adsorption experiments were carried out by agitating 20 mL metformin solution with 3 mg GO at 130 rpm, 303 K in a thermostatic rotary shaker for 160 min. The pH of the solution was adjusted with 0.01–1.0 M HCl or NaOH solution on a digital pH meter (PHS-3C). The mixture was separated by filtering through 0.45 μm membrane filters after adsorption (Xu et al., 2012; Wang et al., 2014).

The residual metformin concentration was measured by UV spectrophotometer (UV-2550, SHIMADZU, Japan) at 232 nm (Sharma et al., 2016). The amount of metformin adsorbed onto GO at the specific time was calculated using the following equation:

$$q_e = \frac{(C_0 - C_e)V}{m} \quad (1)$$

where q_e is the adsorption quantity (mg g^{-1}); C_0 and C_e is the initial and equilibrium concentrations of metformin in solution (mg L^{-1}); V is the volume of solution (L), and m is the mass of GO (mg).

The isotherm experiments were conducted by varying initial concentrations from 8 to 40 mg L^{-1} at three different temperatures (288, 303 and 318 K), and pH value was 6.0. The contact time was set as 160 min to ensure adsorption equilibrium, and the other parameters kept constant.

Kinetic experiments were carried out using 10 mg L^{-1} metformin solution containing 3 mg GO for a period of 160 min at 303 K. Samples were collected at different pre-determined time intervals to evaluate uptake of metformin. The other parameters kept constant.

The effect of pH on the adsorption properties was carried out by varying pH value from 4.0 to 11.0. The other parameters kept the same with above experiments. The concentration of metformin was 10 mg L^{-1}.

The ionic strength experiments were conducted by adding various NaCl concentrations, varying from 0 to 0.1 M, into reaction system, and pH value was 6.0. The concentration of metformin was 10 mg L^{-1}.

In order to investigate the effect of different background electrolyte ions, batch competitive adsorption were studied in the presence of various anions (NO_3^-, SO_4^{2-}, Cl^-) and cations (Na^+, K^+, Mg^{2+} and Ca^{2+}) at the concentration of 0.01 M. The experiment was conducted by adding 3 mg GO in 10 mg L^{-1} of metformin solution with desired anions and cations at pH 6.0 for 160 min. The other parameters kept constant.

2.4. Desorption experiment

Sodium hydroxide was applied to be the desorption medium in the desorption experiment. The GO which had been used to adsorb metformin was washed by 0.2 M NaOH solution at room temperature. Then the adsorbent was washed several times by Milli-Q water and dried to reuse.

3. Results and discussion

3.1. GO characterization

Fig. 1a and b showed the SEM and TEM images of GO. It was apparent that GO displayed many wrinkles on the surface and owned a layered structure, which could contribute to increasing the specific surface area and adsorption capacity of GO.

The XPS spectrums showed the presence of C and O element in the GO at the binding energy of 286.81 eV and 532.52 eV (Fig. 1c). The ratio of carbon content to oxygen content (C/O) for GO was 1.843, which implied the abundance of oxygen-containing functional groups. It showed that the majority of oxygen-containing groups were C-O and C═O (Fig. 1c). These function groups were expected to form strong bonds with metformin on the GO surfaces. The C1s XPS spectrum of GO was shown in Fig. 1d. It was found that four different peaks centered at 284.5, 286.2, 287.8, and 289.0 eV, corresponding to the C═C/C-C, C-O, C═O and O-C═O, respectively (Zhao et al., 2011a), which confirmed that GO has been successfully oxidized via oxidizing reaction. The synthesized GO also presented high specific surface area (108.71 m^2/g) and pore diameter (2.44 nm), which was proved by the BET analysis, and this would be beneficial to the uptake of contaminants. The specific area of GO was much higher than that of graphite (4.5 m^2 g^{-1}) (Zhu and Pignatello, 2005), indicating a good exfoliation degree has been obtained. The reason why the specific area was lower than that of theoretical degree (2620 m^2 g^{-1}) may be that the incomplete exfoliation and the agglomerations of grapheme oxide layers during the process of preparation.

The internal structures of GO and graphite were also examined by XRD and the results were shown in Fig. 1e. From the XRD patterns of GO, a sharp diffraction peak at $2\theta = 10.04^\circ$ (d = 0.88 nm), which was corresponded to the typical diffraction peak of GO, was attributed to the (002) plane. On the contrary, there was a intense peak at 26.50° (d = 0.34 nm) for graphite. The peak at a lower degree could be related to longer distances among the atoms, which suggested that the adjacent layers of the GO were placed in longer distances between one another than those of graphite. The increase of the distances after graphite modification might be the introduction of the abundant oxygen-containing functional groups on the surfaces of GO (Waltman et al., 1993; McAllister et al., 2007; Lee et al., 2015). These results were corresponded with the XPS characteristic.

3.2. Adsorption kinetics

The contact time on metformin adsorption onto GO was one of the main factors, which determined the residence time of uptake at the solid-liquid interface (Mercer and Tobiason, 2008). Thus, the adsorption kinetics must be studied to obtain the optimum contact time. In this study, Fig. 2 showed the time dependence of metformin on GO. Clearly, the removal efficiency reached almost 80% within 20 min, and a slower adsorption until the adsorption equilibrium was obtained in approximately 160 min. The adsorption process was very rapid and efficient, which corresponded with the relatively high k_1 (0.232 min^{-1}) and k_2 (0.007 g mg^{-1} min^{-1}) values in the pseudo-first-order and the pseudo-second-order model. The rapid adsorption rate might be attribute to the sufficiency of active sites and the absence of internal diffusion resistance during the first 20 min (Jiang et al., 2017).

The experimental data was simulated with pseudo-first-order model and pseudo-second-order model, respectively. Fig. 2 exhibited that the curves of the pseudo-first-order and the pseudo-second-order models fitted with kinetic sorption data of metformin adsorption. Detailed information about these models was provided in the Supplementary Material.

After being fitted by the two models, the calculated parameters were listed in Table 1. It was apparent that the pseudo-second-order model (0.980) showed better correlation coefficients (R^2) than the pseudo-first-order model (0.924). Furthermore, the calculated q_e (47.100 mg of metformin g^{-1} GO) value of the pseudo-second-order model was more agreeable to the experimental data better than that of the pseudo-first-order model (Jin et al., 2015). Thus, it could be concluded that the pseudo-second-order model fitted the adsorption process better than the pseudo-first-order model, suggesting that the adsorption rate depended on chemisorption (Hu et al., 2011b; Wu et al., 2016). The result corresponded

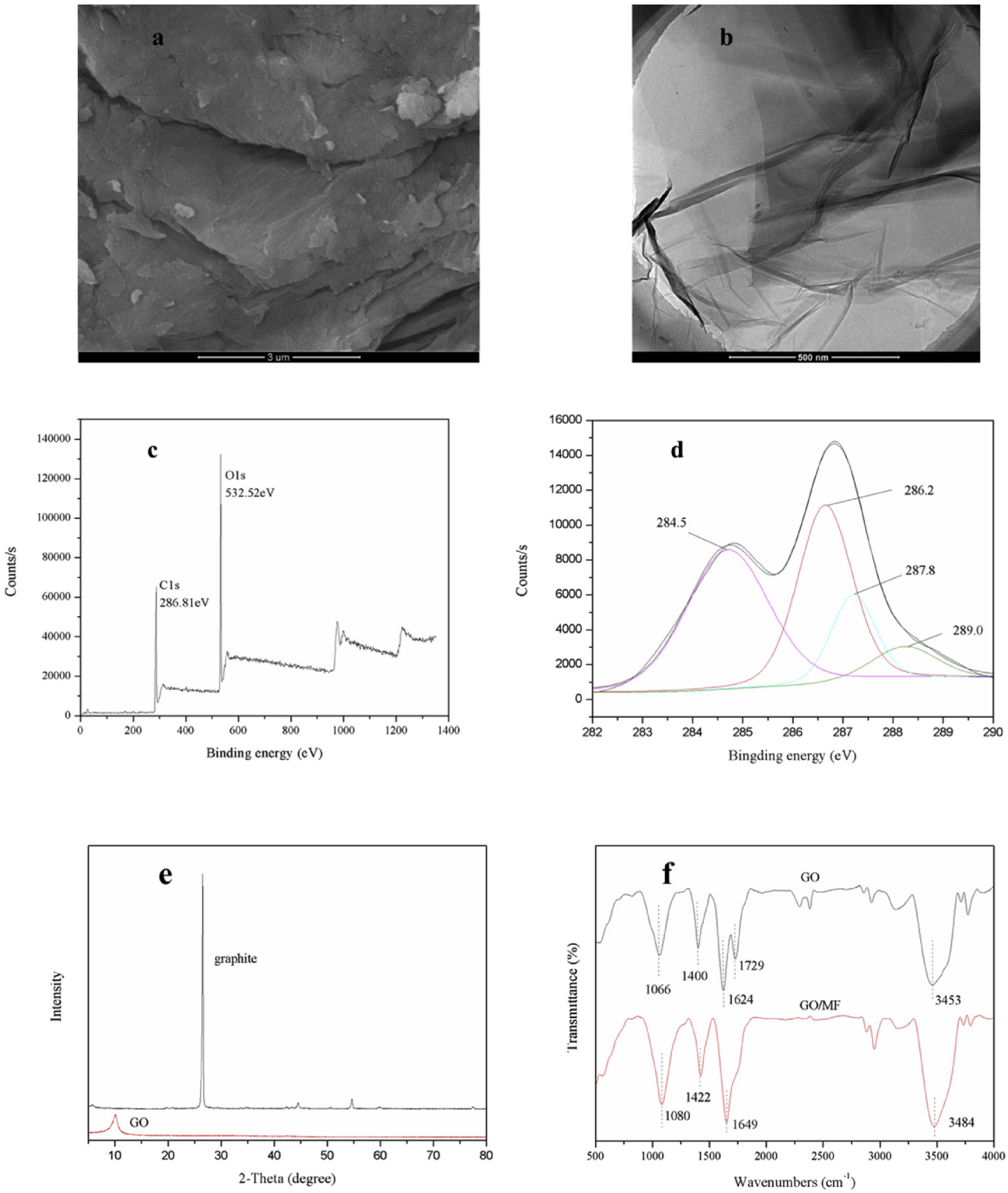

Fig. 1. (a) SEM image of GO; (b) TEM image of GO; (c) XPS survey spectra of GO; (d) C1s core level spectra of GO; (e) XRD patterns of GO and graphite; (f) FTIR spectra of GO before and after metformin adsorption.

with the previous reports (Jiang et al., 2016).

3.3. Adsorption isotherm and thermodynamics

Batch adsorption isotherm experiments were carried out to study the adsorption behaviors in solid and liquid phase at equilibrium, and the results were displayed in Fig. 3. Langmuir and Freundlich isotherm model were the most common models to simulate the adsorption isotherm curve. As for Langmuir model, there was an assumption which the surface of adsorbent had finite

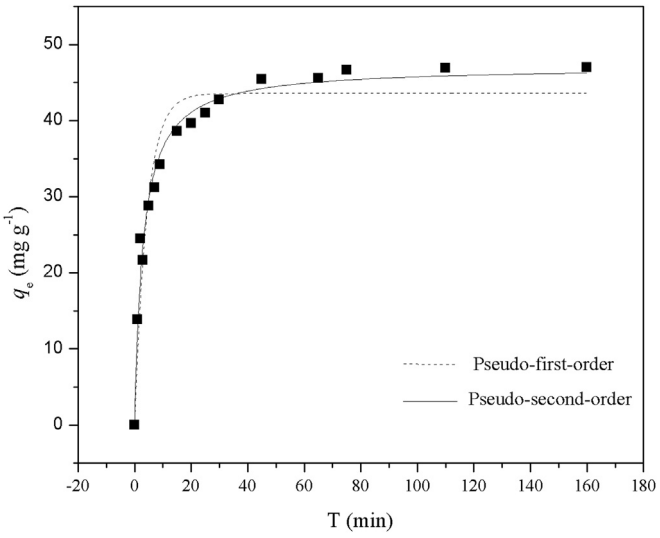

Fig. 2. Kinetics of metformin adsorption onto GO at 303 K, pH = 6.0.

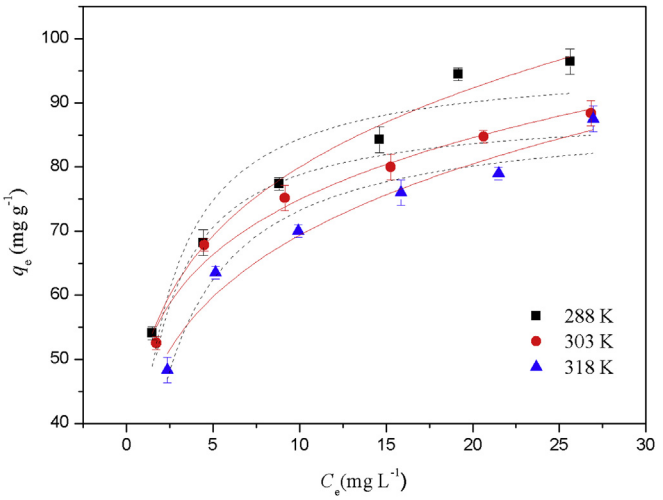

Fig. 3. Adsorption isotherms of metformin by GO at three different temperatures: t = 160 min, pH = 6.0.

adsorption sites, and the adsorption process only occurred by specific homogeneous adsorption without any interaction between the adsorbed GO and pollutants (Wang et al., 2013). By contrast, Freundlich model suggested that adsorption take place on a heterogeneous surface without saturation of adsorbent binding sites (Repo et al., 2010). Detailed information about these models was provided in the Supplementary Material.

The parameters calculated from the two models were listed in Table 2. It could be seen obviously that the correlation coefficient (R^2) values of the Freundlich model were higher than the values of the Langmuir model. The results proved that the adsorption behaviors of metformin onto GO was in compliance with the Freundlich model, and the adsorption process took place on a heterogeneous surface without saturation of adsorbent binding sites. The high values of K_F (49.622, 50.060 and 42.287) indicated that GO had a high adsorption capacity and affinity for metformin. Moreover, the constants n of Freundlich model at three temperatures were 4.824, 5.713 and 4.656, respectively. The n values were more than 1 and less than 10, implying that favorable adsorption was for metformin onto GO at all temperatures studied.

From Table 2, it could also be observed apparently that the highest adsorption capacity in the investigated range was obtained at 288 K. There was a relatively lower adsorption capacity at higher temperature, which suggested that the removal of metformin were promoted at lower temperature.

Thermodynamic parameters were evaluated to confirm the adsorption nature of metformin onto GO (Table S1). These parameters, including standard free-energy change (ΔG^0), standard enthalpy change (ΔH^0), and standard entropy change (ΔS^0), were calculated from the experimental data via relative equations as described in Supplementary Material.

The values of ΔG^0 were negative at all temperatures, which indicated that the adsorption was spontaneous. The adsorption reaction was exothermic according to the negative ΔH^0 value, which was in good agreement with the result showed in Fig. 3 that the adsorption of metformin decreased with the increase in temperature. In addition, the positive ΔS^0 value revealed increased randomness at adsorbate–adsorbent interface during the adsorption progress.

3.4. Effect of initial solution pH

The effect of pH on metformin adsorption by GO was shown in Fig. 4a, which indicated that the adsorption process was sensitive to the varying pH values. It was observed that the uptake of metformin increased when the pH value changed from 4.0 to 6.0, and then decreased with the pH increased from 6.0 to 11.0. These phenomena might be attribute to the change of the surface charge of GO and the speciation of metformin at different pH values.

The zeta potentials of GO under various pH (4.0–11.0) were investigated and the results could be seen in Fig. 4b. It showed that GO had a net negative charge and kept decreasing with the increase of pH. These results indicated that GO was always negatively charged under the condition, and it might hold great promise for positively charged contaminant.

It should be pointed that metformin has two distant pK_a values (pK_1 = 2.8, pK_2 = 11.6), corresponding to the biprotonated/monoprotonated, and monoprotonated/neutral form conversions, respectively. Considering different pKa values and species of metformin, the monoprotonated forms might increase from 4.0 to 6.0, then decreased at higher pH values. Thus, the amount changes of the monoprotonated form could lead to a decline in electron–accept ability of metformin and weaker interactions of so-called π–π interactions between graphene oxide and metformin. Furthermore, the electrostatic interactions between the negative charged GO and the positive charged metformin might not be the main adsorption force.

Table 1
Kinetic parameters for adsorption of metformin onto GO.

$q_{e,exp}$	Pseudo-first-order			Pseudo-second-order		
	$q_{e,1}$ (mg of metformin g^{-1} GO)	k_1 (min^{-1})	R^2	$q_{e,2}$ (mg of metformin g^{-1} GO)	k_2 (g mg^{-1} min^{-1})	R^2
	43.586 ± 1.281	0.232 ± 0.031	0.924	47.100 ± 0.856	0.007 ± 0.001	0.980

Table 2
Constants and correlation coefficients of Langmuir model and Freundlich model for metformin adsorption onto GO.

T (K)	Langmuir model			Freundlich model		
	q_m (of mg metformin g^{-1} GO)	K_L (L mg^{-1})	R^2	K_F (L mg^{-1})	n	R^2
288	96.748 ± 4.521	0.681 ± 0.183	0.869	49.622 ± 1.602	4.82 ± 0.289	0.985
303	89.099 ± 2.013	0.763 ± 0.107	0.957	50.060 ± 1.760	5.713 ± 0.439	0.975
318	88.517 ± 3.060	0.478 ± 0.086	0.935	42.287 ± 2.385	4.656 ± 0.456	0.961

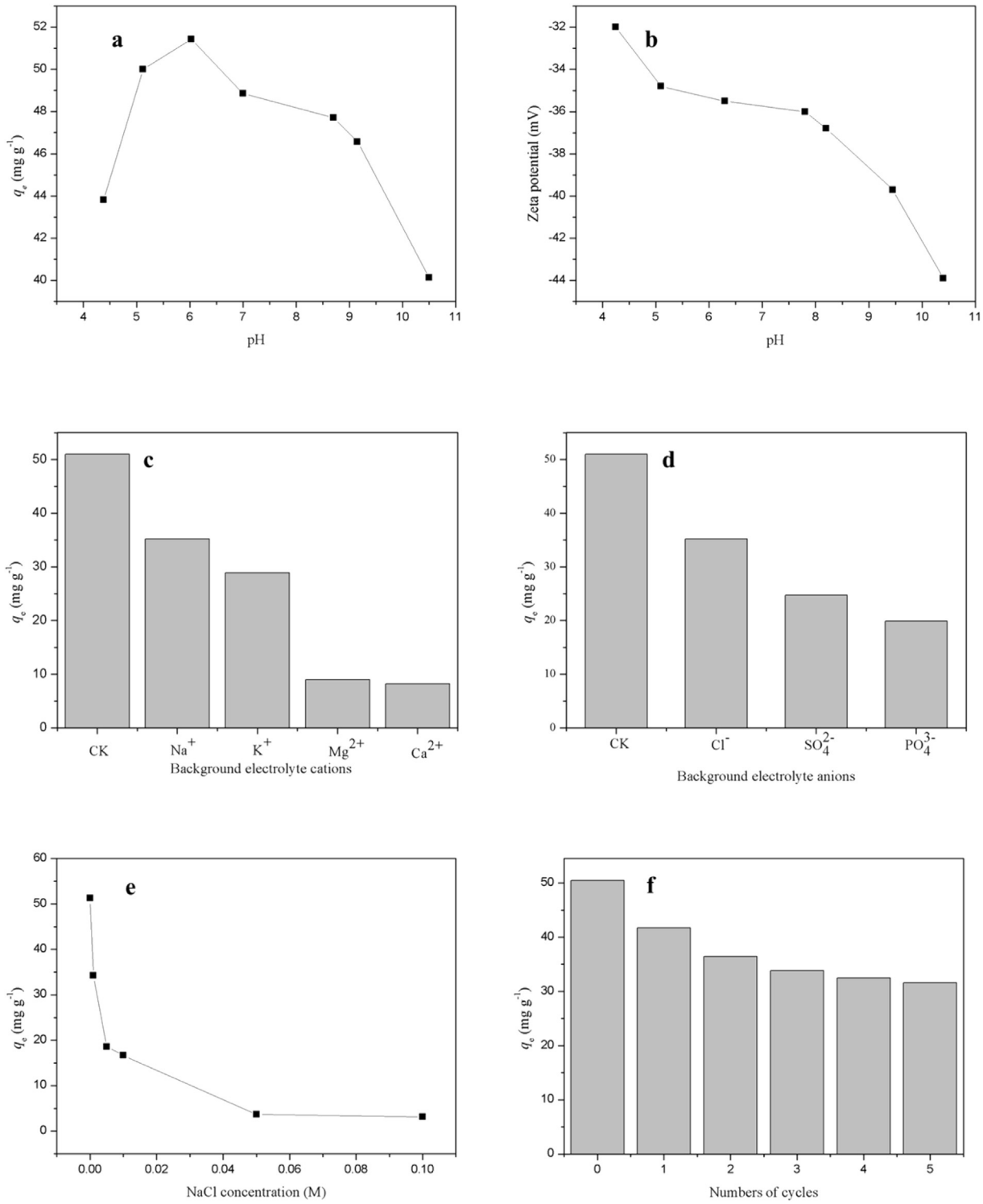

Fig. 4. (a) Effect of the solution pH; (b) Zeta potentials; (c) Effect of background electrolyte cations; (d) Effect of background electrolyte anions; (e) Effect of ionic strength; (f) Adsorption/desorption cycles: T = 303 K, t = 160 min, pH = 6.0.

3.5. Effect of background electrolyte

In order to examine the effect of background electrolyte on the adsorption capacity, batch experiments were carried out. The results were presented in Fig. 4c and d. It was obvious to find that there was a negative effect on the metformin adsorption when the reaction occurred in the presence of various background electrolytes, including both anions and cations. It could be found that the impact of divalent cations (Ca^{2+} and Mg^{2+}) on the metformin adsorption was larger than monovalent cations (Na^{+} and K^{+}). This might be attributed to higher polarizing power of divalent cations (Hu et al., 2014b), which further resulted in easily and strongly occupying more adsorption sites by electrostatic attraction on GO than Na^{+} and K^{+}. There was also a decrease of metformin adsorption on GO in the presence of anions, the adsorption of metformin under the same pH value was in the following sequence: $CK > Cl^{-} > SO_4^{2-} > PO_4^{3-}$.The phenomenon might be explained by the competition of higher concentration of Na^{+} ions with the metformin for adsorption sites (Hu et al., 2014b), for the adsorption experiments were studied in the presence of 0.01 M NaCl, Na_2SO_4, and Na_3PO_4 solutions, respectively. Thus, lower adsorption on the GO surfaces was achieved with the decrease of valence.

3.6. Effect of ionic strength

Considering the complexity of water resources, various ionic strength might influence the uptake capacity of GO to metformin. Therefore, the effect of ionic strength was conducted by batch experiments at different concentrations of NaCl, and the obtained results were shown in Fig. 4e. It was found that the adsorption capacity reduced with increasing concentration of NaCl from 0 to 0.1 M. This phenomenon could be explained by following possibilities: (i) there might be a great detriment in active coefficients of metformin, which limited their migrating to GO surfaces; (ii) the competitive adsorption between Na^{+} ions and metformin was helpful to decrease the uptake capacity of GO; (iii) the increased ionic strength reduced the electrostatic repulsions between GO, resulting in the aggregation of GO particles (Hu et al., 2014a; Jiang et al., 2016).

3.7. Desorption experiment

Desorption experiments were carried out to study the reusability and cost effectiveness of GO in this study. As it shown in Fig. 4f, the adsorption capacity of GO decreased with the increase of cycles. The adsorption capacity of metformin onto GO was 50.47 mg of metformin g^{-1} GO in the first circle, and after five cycles it could still remain at 31.60 mg of metformin g^{-1} GO. Therefore, it could be concluded that GO could be considered as an economical adsorbent. The decrease of specific surface area and functional groups might contribute to the lower adsorption capacity of metformin onto GO (Pavagadhi et al., 2013).

3.8. Adsorption mechanism

Due to the large quantities of oxygen-containing functional groups and aromatic rings on the surface, GO established π-electron acceptor or donor properties (Zhou et al., 2015; Yu et al., 2016). Due to the presence of delocalized π-electron system, the theoretical calculations have predicted a quasiplanar structure for the two monoprotonated forms. Thus, metformin could be considered as a good candidate for stabilizing the so-called π−π interactions, for instance, with the aromatic rings involved in graphene oxide. (Hernández et al., 2015). Besides, hydrogen bonds could also occur between amines of metformin and oxygen-containing groups in GO. According to our study, the electrostatic interactions between the negative charged GO and the positive charged metformin might not be the main adsorption force during the adsorption process.

In order to investigate the molecular interaction of metformin with GO, the FTIR spectra of GO before (GO) and after metformin adsorption (GO/MF) were shown in Fig. 1f. Several characteristic peaks were observed in the GO spectrum, such as 3453 cm^{-1} (O-H), 1729 and 1400 cm^{-1} (C═O), 1624 cm^{-1} (C═C), and 1066 cm^{-1} (C-O-C) (Jin et al., 2015). It was obvious to find that there were large amount of oxygen-containing functional groups existed on GO surface, the result was consistent with XPS analysis. However, the characteristic peak centered at 1624 cm^{-1} slightly shifted to 1635 cm^{-1} after adsorption. This could be corresponded to C═C skeletal vibration, owing to the so-called π−π interaction between metformin and GO. Moreover, the peaks of the O-H bending vibration and epoxy C-O-C bending vibration of GO migrated to 3484 cm^{-1} and 1080 cm^{-1}, respectively. The peak of C═O (1729 cm^{-1}) could not be found in the spectrum after adsorption. These might suggest that hydrogen bonds formed after metformin adsorption. Based on the above analysis, the so-called π−π interactions and hydrogen bonds might mainly be the probable adsorption mechanism. The adsorption mechanism could be illustrated by Fig. S1.

4. Conclusions

This research explored the possibility of using GO as an adsorbent to remove metformin from water under different concentrations and pH values. GO exhibited high adsorption capacity even under the existence of other surrounding conditions, including pH, ionic strength, temperature, and background electrolyte. The highest adsorption capacity in the investigated range (q_m) of GO was at 288 K and pH 6.0. The isotherm parameters and kinetics could be well described by the Freundlich isotherm and pseudo-second-order kinetic model, respectively. The adsorption process was exothermic and spontaneous, which was confirmed by the thermodynamic study. GO showed excellent adsorption capacity after numerous desorption/adsorption cycles. The excellent adsorption capacity of GO for metformin might mainly due to so-called π−π interactions and hydrogen bonds. Thus, GO could be an efficient and potential adsorbent for metformin removal.

Acknowledgements

This work was supported by the National Natural Science Foundation of China (Grant No. 41271332, 51521006); and the International S&T Cooperation Program of China (project contract NO: 2015DFG92750).

Appendix A. Supplementary data

Supplementary data related to this article can be found at http://dx.doi.org/10.1016/j.chemosphere.2017.03.071.

References

Blair, B.D., Crago, J.P., Hedman, C.J., Treguer, R.J., Magruder, C., Royer, L.S., Klaper, R.D., 2013. Evaluation of a model for the removal of pharmaceuticals, personal care products, and hormones from wastewater. Sci. Total Environ. 444, 515–521.

Chang, H., Wu, H., 2013. Graphene-based nanocomposites: preparation, functionalization, and energy and environmental applications. Energy Environ. Sci. 6, 3483–3507.

Crago, J., Bui, C., Grewal, S., Schlenk, D., 2016. Age-dependent effects in fathead minnows from the anti-diabetic drug metformin. Gen. Comp. Endocr. 232, 185–190.

Cui, H., Schröder, P., 2016. Uptake, translocation and possible biodegradation of the

antidiabetic agent metformin by hydroponically grown Typha latifolia. J. Hazard. Mater. 308, 355–361.
Escher, B.I., Baumgartner, R., Koller, M., Treyer, K., Lienert, J., McArdell, C.S., 2011. Environmental toxicology and risk assessment of pharmaceuticals from hospital wastewater. Water Res. 45, 75–92.
Fakhri, A., January 2017. Adsorption characteristics of graphene oxide as a solid adsorbent for aniline removal from aqueous solutions: kinetics, thermodynamics and mechanism studies. J. Saudi Chem. Soc. 21 (Suppl. 1), S52–S57.
Gao, Y., Li, Y., Zhang, L., Huang, H., Hu, J., Shah, S.M., Su, X., 2012. Adsorption and removal of tetracycline antibiotics from aqueous solution by graphene oxide. J. Colloid Interface Sci. 368, 540–546.
Gu, W., Sun, C.-j., Liu, Q., Cui, H.-x., 2009. Adsorption of avermectins on activated carbon: equilibrium, kinetics, and UV-shielding. Trans. Nonferr. Metal. Soc. 19, s845–s850.
Gupta, V.K., Singh, P., Rahman, N., 2004. Adsorption behavior of Hg(II), Pb(II), and Cd(II) from aqueous solution on Duolite C-433: a synthetic resin. J. Colloid Interface Sci. 275, 398–402.
Gupta, V.K., Srivastava, S.K., Mohan, D., Sharma, S., 1998. Design parameters for fixed bed reactors of activated carbon developed from fertilizer waste for the removal of some heavy metal ions. Waste Manag. 17, 517–522.
Hernández, B., Pflüger, F., Kruglik, S.G., Cohen, R., Ghomi, M., 2015. Protonation–deprotonation and structural dynamics of antidiabetic drug metformin. J. Pharm. Biomed. 114, 42–48.
Hu, X.-j., Liu, Y.-g., Zeng, G.-m., Wang, H., Hu, X., Chen, A.-w., Wang, Y.-q., Guo, Y.-m., Li, T.-t., Zhou, L., 2014a. Effect of aniline on cadmium adsorption by sulfanilic acid-grafted magnetic graphene oxide sheets. J. Colloid Interface Sci. 426, 213–220.
Hu, X.-j., Liu, Y.-g., Zeng, G.-m., You, S.-h., Wang, H., Hu, X., Guo, Y.-m., Tan, X.-f., Guo, F.-y., 2014b. Effects of background electrolytes and ionic strength on enrichment of Cd(II) ions with magnetic graphene oxide–supported sulfanilic acid. J. Colloid Interface Sci. 435, 138–144.
Hu, X.-j., Wang, J.-s., Liu, Y.-g., Li, X., Zeng, G.-m., Bao, Z.-l., Zeng, X.-x., Chen, A.-w., Long, F., 2011a. Adsorption of chromium (VI) by ethylenediamine-modified cross-linked magnetic chitosan resin: isotherms, kinetics and thermodynamics. J. Hazard. Mater. 185, 306–314.
Hu, X.-j., Wang, J.-s., Liu, Y.-g., Li, X., Zeng, G.-m., Bao, Z.-l., Zeng, X.-x., Chen, A.-w., Long, F., 2011b. Adsorption of chromium (VI) by ethylenediamine-modified cross-linked magnetic chitosan resin:isotherms, kinetics and thermodynamics. J. Hazard. Mater. 185, 306–314.
Hu, X., Wang, H., Liu, Y., 2016. Statistical analysis of main andinteraction effects on Cu(II) and Cr(VI) decontamination by nitrogen–doped magnetic graphene oxide. Sci. Rep. U. K. 6, 34378.
Jiang, L.-h., Liu, Y.-g., Zeng, G.-m., Xiao, F.-y., Hu, X.-j., Hu, X., Wang, H., Li, T.-t., Zhou, L., Tan, X.-f., 2016. Removal of 17β-estradiol by few-layered graphene oxide nanosheets from aqueous solutions: external influence and adsorption mechanism. Chem. Eng. J. 284, 93–102.
Jiang, L., Liu, Y., Liu, S., Hu, X., Zeng, G., Hu, X., Liu, S., Liu, S., Huang, B., Li, M., 2017. Fabrication of β-cyclodextrin/poly (l-glutamic acid) supported magnetic graphene oxide and its adsorption behavior for 17β-estradiol. Chem. Eng. J. 308, 597–605.
Jin, Z., Wang, X., Sun, Y., Ai, Y., Wang, X., 2015. Adsorption of 4-n-nonylphenol and bisphenol-a on magnetic reduced graphene oxides: a combined experimental and theoretical studies. Environ. Sci. Technol. 49, 9168–9175.
Kim, M., Guerra, P., Shah, A., Parsa, M., Alaee, M., Smyth, S.A., 2014. Removal of pharmaceuticals and personal care products in a membrane bioreactor wastewater treatment plant. Water Sci. Technol. 69, 2221–2229.
Kyzas, G.Z., Fu, J., Lazaridis, N.K., Bikiaris, D.N., Matis, K.A., 2015. New approaches on the removal of pharmaceuticals from wastewaters with adsorbent materials. J. Mol. Liq. 209, 87–93.
Lee, B.-M., Seo, Y.-S., Hur, J., 2015. Investigation of adsorptive fractionation of humic acid on graphene oxide using fluorescence EEM-PARAFAC. Water Res. 73, 242–251.
Lu, X., Shao, Y., Gao, N., Chen, J., Zhang, Y., Wang, Q., Lu, Y., 2016. Adsorption and removal of clofibric acid and diclofenac from water with MIEX resin. Chemosphere 161, 400–411.
McAllister, M.J., Li, J.-L., Adamson, D.H., Schniepp, H.C., Abdala, A.A., Liu, J., Herrera-Alonso, M., Milius, D.L., Car, R., Prud'homme, R.K., Aksay, I.A., 2007. Single sheet functionalized graphene by oxidation and thermal expansion of graphite. Chem. Mater. 19, 4396–4404.
Mercer, K.L., Tobiason, J.E., 2008. Removal of arsenic from high ionic strength solutions: effects of ionic strength, pH, and preformed versus in situ formed HFO. Environ. Sci. Technol. 42, 3797–3802.
Mittal, A., Kaur, D., Malviya, A., Mittal, J., Gupta, V.K., 2009a. Adsorption studies on the removal of coloring agent phenol red from wastewater using waste materials as adsorbents. J. Colloid Interface Sci. 337, 345–354.
Mittal, A., Mittal, J., Malviya, A., Gupta, V.K., 2009b. Adsorptive removal of hazardous anionic dye "Congo red" from wastewater using waste materials and recovery by desorption. J. Colloid Interface Sci. 340, 16–26.
Mittal, A., Mittal, J., Malviya, A., Gupta, V.K., 2010a. Removal and recovery of Chrysoidine Y from aqueous solutions by waste materials. J. Colloid Interface Sci. 344, 497–507.
Mittal, A., Mittal, J., Malviya, A., Kaur, D., Gupta, V.K., 2010b. Decoloration treatment of a hazardous triarylmethane dye, Light Green SF (Yellowish) by waste material adsorbents. J. Colloid Interface Sci. 342, 518–527.
Moradi, O., Gupta, V.K., Agarwal, S., Tyagi, I., Asif, M., Makhlouf, A.S.H., Sadegh, H., Shahryari-ghoshekandi, R., 2015. Characteristics and electrical conductivity of graphene and graphene oxide for adsorption of cationic dyes from liquids: kinetic and thermodynamic study. J. Ind. Eng. Chem. 28, 294–301.
Neamțu, M., Grandjean, D., Sienkiewicz, A., Le Faucheur, S., Slaveykova, V., Colmenares, J.J.V., Pulgarín, C., de Alencastro, L.F., 2014. Degradation of eight relevant micropollutants in different water matrices by neutral photo-Fenton process under UV254 and simulated solar light irradiation – a comparative study. Appl. Catal. B Environ. 158–159, 30–37.
Niemuth, N.J., Klaper, R.D., 2015. Emerging wastewater contaminant metformin causes intersex and reduced fecundity in fish. Chemosphere 135, 38–45.
Oosterhuis, M., Sacher, F., ter Laak, T.L., 2013. Prediction of concentration levels of metformin and other high consumption pharmaceuticals in wastewater and regional surface water based on sales data. Sci. Total Environ. 442, 380–388.
Pavagadhi, S., Tang, A.L.L., Sathishkumar, M., Loh, K.P., Balasubramanian, R., 2013. Removal of microcystin-LR and microcystin-RR by graphene oxide: adsorption and kinetic experiments. Water Res. 47, 4621–4629.
Ramesha, G.K., Vijaya Kumara, A., Muralidhara, H.B., Sampath, S., 2011. Graphene and graphene oxide as effective adsorbents toward anionic and cationic dyes. J. Colloid Interface Sci. 361, 270–277.
Repo, E., Warchol, J.K., Kurniawan, T.A., Sillanpää, M.E.T., 2010. Adsorption of Co(II) and Ni(II) by EDTA- and/or DTPA-modified chitosan: kinetic and equilibrium modeling. Chem. Eng. J. 161, 73–82.
Rice, S.L., Mitra, S., 2007. Microwave-assisted solvent extraction of solid matrices and subsequent detection of pharmaceuticals and personal care products (PPCPs) using gas chromatography–mass spectrometry. Anal. Chim. Acta 589, 125–132.
Sharma, D., Ojha, H., Pathak, M., Singh, B., Sharma, N., Singh, A., Kakkar, R., Sharma, R.K., 2016. Spectroscopic and molecular modelling studies of binding mechanism of metformin with bovine serum albumin. J. Mol. Struct. 1118, 267–274.
Sitko, R., Turek, E., Zawisza, B., Malicka, E., Talik, E., Heimann, J., Gagor, A., Feist, B., Wrzalik, R., 2013. Adsorption of divalent metal ions from aqueous solutions using graphene oxide. Dalton Trans. 42, 5682–5689.
Tan, X.-f., Liu, S.-b., Liu, Y.-g., Gu, Y.-l., Zeng, G.-m., Hu, X.-j., Wang, X., Liu, S.-h., Jiang, L.-h., 2017. Biochar as potential sustainable precursors for activated carbon production: multiple applications in environmental protection and energy storage. Bioresour. Technol. 227, 359–372.
Tan, X.-f., Liu, Y.-g., Gu, Y.-l., Xu, Y., Zeng, G.-m., Hu, X.-j., Liu, S.-b., Wang, X., Liu, S.-m., Li, J., 2016. Biochar-based nano-composites for the decontamination of wastewater: a review. Bioresour. Technol. 212, 318–333.
Tan, X., Liu, Y., Zeng, G., Wang, X., Hu, X., Gu, Y., Yang, Z., 2015. Application of biochar for the removal of pollutants from aqueous solutions. Chemosphere 125, 70–85.
Tang, T., Lord, J.M., Norman, R.J., Yasmin, E., Balen, A.H., 2012. Insulin-sensitising drugs (metformin, rosiglitazone, pioglitazone, D-chiro-inositol) for women with polycystic ovary syndrome, oligo amenorrhoea and subfertility. Cochrane Db. Syst. Rev. 5. Cd003053.
Terzić, S., Senta, I., Ahel, M., Gros, M., Petrović, M., Barcelo, D., Müller, J., Knepper, T., Martí, I., Ventura, F., Jovančić, P., Jabučar, D., 2008. Occurrence and fate of emerging wastewater contaminants in Western Balkan Region. Sci. Total Environ. 399, 66–77.
Viollet, B., Guigas, B., Sanz Garcia, N., Leclerc, J., Foretz, M., Andreelli, F., 2012. Cellular and molecular mechanisms of metformin: an overview. Clin. Sci. 122, 253–270.
Waltman, R.J., Pacansky, J., Bates, C.W., 1993. X-ray photoelectron spectroscopic studies on organic photoconductors: evaluation of atomic charges on chlorodiane blue and p-(diethylamino)benzaldehyde diphenylhydrazone. Chem. Mater. 5, 1799–1804.
Wang, J., Chen, Z., Chen, B., 2014. Adsorption of polycyclic aromatic hydrocarbons by graphene and graphene oxide nanosheets. Environ. Sci. Technol. 48, 4817–4825.
Wang, T., Liu, W., Xiong, L., Xu, N., Ni, J., 2013. Influence of pH, ionic strength and humic acid on competitive adsorption of Pb(II), Cd(II) and Cr(III) onto titanate nanotubes. Chem. Eng. J. 215–216, 366–374.
Wang, W., Li, X., Yuan, S., Sun, J., Zheng, S., 2016. Effect of resin charged functional group, porosity, and chemical matrix on the long-term pharmaceutical removal mechanism by conventional ion exchange resins. Chemosphere 160, 71–79.
Wu, Z., Yuan, X., Zhang, J., Wang, H., Jiang, L., Zeng, G., 2017. Photocatalytic decontamination of wastewater containing organic dyes by metal-organic frameworks and their derivatives. ChemCatChem 9, 41–64.
Wu, Z., Yuan, X., Zhong, H., Wang, H., Zeng, G., Chen, X., Wang, H., Zhang, L., Shao, J., 2016. Enhanced adsorptive removal of p-nitrophenol from water by aluminum metal-organic framework/reduced graphene oxide composite. Sci. Rep. U. K. 6, 25638.
Xu, J., Wang, L., Zhu, Y., 2012. Decontamination of bisphenol a from aqueous solution by graphene adsorption. Langmuir ACS J. Surfaces Colloids 28, 8418–8425.
Yao, Y., Xu, F., Chen, M., Xu, Z., Zhu, Z., 2010. Adsorption behavior of methylene blue on carbon nanotubes. Bioresour. Technol. 101, 3040–3046.
Yoon, Y., Westerhoff, P., Snyder, S.A., Esparza, M., 2003. HPLC-fluorescence detection and adsorption of bisphenol A, 17β-estradiol, and 17α-ethynyl estradiol on powdered activated carbon. Water Res. 37, 3530–3537.
Yu, S., Wang, X., Ai, Y., Tan, X., Hayat, T., Hu, W., Wang, X., 2016. Experimental and theoretical studies on competitive adsorption of aromatic compounds on reduced graphene oxides. J. Mater. Chem. A 4, 5654–5662.
Zhao, G., Li, J., Ren, X., Chen, C., Wang, X., 2011a. Few-layered graphene oxide

nanosheets as superior sorbents for heavy metal ion pollution management. Environ. Sci. Technol. 45, 10454–10462.
Zhao, G., Li, J., Ren, X., Chen, C., Wang, X., 2011b. Few-layered graphene oxide nanosheets as superior sorbents for heavy metalion pollution management. Environ. Sci. Technol. 45, 10454–10462.
Zhou, Y., Apul, O.G., Karanfil, T., 2015. Adsorption of halogenated aliphatic contaminants by graphene nanomaterials. Water Res. 79, 57–67.
Zhu, D., Pignatello, J.J., 2005. Characterization of aromatic compound sorptive interactions with black carbon (Charcoal) assisted by graphite as a model. Environ. Sci. Technol. 39, 2033–2041.